

Electrochemical corrosion behavior of novel Cu-containing antimicrobial austenitic and ferritic stainless steels in chloride media

Emeka E. Oguzie · Jibiao Li · Yongqian Liu · Demin Chen · Ying Li · Ke Yang · Fuhui Wang

Received: 7 April 2010/Accepted: 26 May 2010/Published online: 15 July 2010
© Springer Science+Business Media, LLC 2010

Abstract The electrochemical corrosion behavior of novel Cu-containing antibacterial austenitic and ferritic stainless steels in 0.05 mol/L NaCl solution has been investigated by dc polarization and ac impedance measurements and compared with that of the conventional stainless steels. Cu was found to particularly affect the kinetics of the anodic reaction. The corrosion performance of the austenite was greatly improved by Cu addition in the studied anodic potential range, whereas Cu effects on the ferrite showed remarkable sensitivity to the applied potential and improved corrosion resistance only in the low anodic potential range. Three-dimensional presentation of the variable-potential impedance data was employed in analyzing the electrochemical corrosion processes and revealed a close relationship between the impedance parameters and the applied potential. The trends of impedance results agree well with those obtained from potentiodynamic polarization measurements.

Introduction

Extensive applications of stainless steels in medical apparatus, kitchenware, and facilities of food processing have necessitated the development of stainless steels with excellent antibacterial properties. Copper, incorporated in some stainless steels, has been reported to impart antimicrobial activity due to precipitation of epsilon copper on the stainless steel surface, which has a devastating effect on bacterial cells [1]. Interestingly, Cu is also a well known alloying element which is used to improve the resistance to general corrosion of stainless steels. Thus, Cu addition has formed the basis for design of some long-lasting and broad-spectrum antibacterial stainless steels.

The mechanism of the protective effect of added Cu has been widely studied and the generally accepted consensus is that dissolved Cu forms metal deposits in a corroded site, which suppress anodic dissolution. This protective effect depends on the stability of the deposited Cu, though chloride ions are particularly known to diminish this stability [2–5]. The effect of alloying Cu on corrosion performance has much contradiction between austenitic and ferritic stainless steels. According to Ujiro et al. [2], suppression of the anodic dissolution by deposited Cu is more effective for ferritic than for austenitic stainless steels. For the former, they observed a powdery morphology which covered the steel surface uniformly unlike the austenitic steel which formed granular corrosion product non-uniformly over the steel surface. Accordingly, the deposited Cu is in more intimate contact with the ferrite surface and exerts a greater protective effect. On the other hand, Zhang et al. [1] on the basis of AFM results reported the presence of spherical Cu deposits, distributed uniformly on the surface of austenitic stainless steels, even after polishing. Moreover, for ferritic stainless steels they observed that the

E. E. Oguzie (✉) · J. Li · Y. Li · F. Wang (✉)
State Key Laboratory for Corrosion and Protection,
Institute of Metal Research, Chinese Academy of Sciences,
62 Wencui Road, Shenyang 110015, China
e-mail: oguziemeka@yahoo.com

F. Wang
e-mail: fhwang@imr.ac.cn

Y. Liu · D. Chen · K. Yang
Center for Engineering Materials, Institute of Metal Research,
Chinese Academy of Sciences, 72 Wenhua Road,
Shenyang 110016, China

E. E. Oguzie
Electrochemistry and Materials Science Research Laboratory,
Department of Chemistry, Federal University of Technology
Owerri, PMB 1526 Owerri, Nigeria

precipitation of Cu also brings about significant degradation of corrosion resistance in chloride solution [6]. Such glaring discrepancies belie the complex role of Cu on the corrosion performance of stainless steels and provide sufficient motivation for continued and more detailed investigations.

Electrochemical methods find wide application in corrosion science [7–10] and the electrochemical responses of the metal/corrodent interface exhibits the characteristic signatures of electronic, chemical, and mass transfer processes, which are often characterized by means of potentiodynamic polarization and electrochemical impedance spectroscopy. The corrosion current density and impedance spectra vary with the electrode potential and as a result the comprehensive characterization of the interface by the electrochemical response should normally reflect the potential dependence of both the dc current response as well as that of the real and imaginary ac impedance components. However, due to the complexity of acquisition of the multidimensional impedance dependencies, impedance data are often acquired at a constant potential, thus neglecting any additional information that could be realized from considering the dependence of the electrochemical impedance spectra on electrode potential.

In this report, we demonstrate the application of potentiodynamic polarization and variable-potential impedance measurements to investigate the effect of Cu addition on the corrosion behavior of novel antimicrobial austenitic and ferritic stainless steels in chloride medium. The Cu contents have been optimized to give the best long term, broad spectrum antibacterial efficacy (>99% for organism such as *Bacillus coli*, *Staphylococcus aureus*, and *Candida albicans*; and >80% efficacy was reported for *Bacillus sublis*) [11–13]. Though this system has been extensively investigated using a number of techniques, there is as yet no generally accepted consensus on the specific roles of the Cu additives. We have attempted to access new information on the dependencies of the impedance response on electrode potential, which, together with the potentiodynamic polarization performance, enables acquisition plus analysis of the potential dependence of both the dc and the ac electrochemical responses.

Experimental

We had previously prepared a range of Cu-containing antimicrobial stainless steels and determined the influence of Cu concentration on antimicrobial efficacy [11–13]. We have selected the Cu-containing austenite and ferrite with the most pronounced antimicrobial activity for electrochemical investigation in this study and compared the electrochemical behavior of each with that of the conventional stainless steel (without Cu).

Table 1 Composition of the Cu-containing austenitic and ferritic stainless steel (mass fraction %)

Element	C	Cr	Si	Mn	Ni	S	P	Cu
Austenite	0.025	18.8	0.8	1.7	9.6	0.007	0.006	3.8
Ferrite	0.03	17.6	0.7	0.6	–	0.008	0.007	1.8

The stainless steel specimens used in this study was an austenitic (304 SS) stainless steel and a ferritic (430 SS) stainless steels. The chemical compositions of the Cu-containing specimens are presented in Table 1. Details of the fabrication (including the heat treatment regimen), microstructure, and antibacterial characterization of the Cu-containing specimens are as previously reported [11–13]. Specimens for corrosion tests were coupons of dimensions; 9 mm × 9 mm × 9 mm polished to # 800 finish with SiC paper and degreased with acetone.

Electrochemical experiments were performed using a PARC PARSTAT-2273 Advanced Electrochemical System operated with Powercorr and Powersine software. The test solution was 0.05 mol/L NaCl, prepared from analytical reagent grade sodium chloride and distilled water. A conventional three-electrode glass cell was used for the experiments. Test coupons of with 0.8 cm² exposed surface area were used as working electrode and a platinum foil as counter electrode. The reference electrode was a saturated calomel electrode (SCE), which was connected via a Luggin's capillary. The working electrodes were always immersed in the test solution for 30 min to attain a stable open circuit potential. Potentiodynamic polarization studies were carried out in the potential range –1100 to 600 mV at a scan rate of 0.333 mV s^{–1}. Electrochemical impedance spectroscopy (EIS) measurements were obtained by holding the samples at a series of specified potentials in the frequency range 100 kHz–1 Hz, with a signal amplitude perturbation of 5 mV. Spectra analyses were performed using Zsimpwin software, also supplied by PARC. All experiments were undertaken in stagnant aerated solutions at 30 ± 1 °C. All experiments were run at least three times and the data always showed good reproducibility.

Results and discussion

Open circuit potential

The open-circuit potentials of the conventional and Cu-containing stainless steel specimens were measured as a function of time in 0.05 mol/L NaCl solution at 30 °C. Figure 1 is a plot of this data for $t \leq 1000$ s, which is enough time for the specimens attain stable open-circuit potentials. For the austenite (Fig. 1a), we observe that the

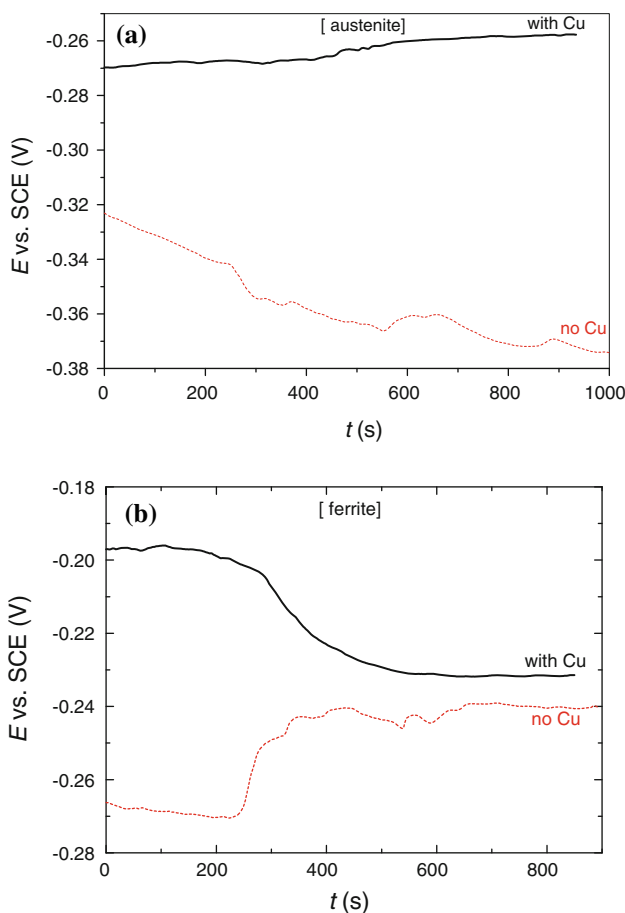


Fig. 1 Open circuit potential–time variation of **a** austenitic and **b** ferritic stainless steels, with and without Cu addition in 0.05 mol/L NaCl solution

potential of the Cu-containing specimen is always more positive than for the Cu-free specimen. In the former case, E increased slightly from -270 mV to -260 mV and for the latter, E decreased from -324 mV to -375 mV. This suggests that Cu had a marked influence on the anodic dissolution process. Figure 1b shows distinctive discrepancies in the open-circuit potential behavior of the ferritic specimens at the initial periods of immersion, which could be attributed to an influence of the added Cu. For both specimens, potential remained more or less stable up to about 250 s and thereafter increased from -270 mV to -240 mV for the Cu-free specimen (implying formation of a protective corrosion product layer) and decreased from -220 mV to -230 mV for the Cu-containing specimen. The decrease in potential could be related to Cu dissolution at the initial stages of immersion, due probably to the low solubility of Cu in ferrite as earlier reported by Banas and Mazurkiewicz [14]. The close agreement of the attained stable potentials possibly implies that Cu only slightly influenced the kinetics of the anodic reaction.

Potentiodynamic polarization behavior

Figure 2 illustrates the typical anodic and cathodic polarization curves of the austenitic (Fig. 2a) and ferritic (Fig. 2b) stainless steels without and with Cu addition in 0.05 mol/L NaCl solution at 30 °C. The corresponding electrochemical parameters are listed in Table 2 [15]. All of the samples obviously underwent active dissolution with no distinctive transition to passivation within the studied potential range. Although Fig. 2a shows similar polarization characteristics for the austenite without and with Cu, there are clear indications that the Cu-containing specimen has a higher resistance to corrosion: the corrosion potential is more positive than that of the Cu-free specimen and the anodic current density is lower within the investigated potential region. As a matter of fact, Table 2 reveals that the magnitude of the polarization resistance (R_p) for the Cu-free austenite is about 8 times higher than that of the Cu-containing specimen. As R_p values are inversely proportional to the corrosion current density according to

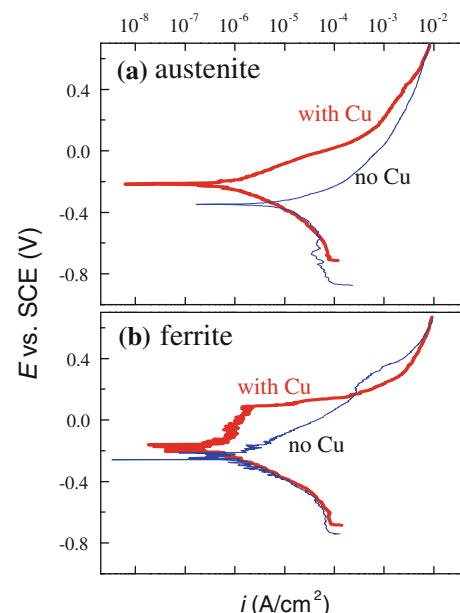


Fig. 2 Potentiodynamic polarization curves of **a** austenitic and **b** ferrite stainless steels, with and without Cu addition in 0.05 mol/L NaCl solution

Table 2 Polarization parameters of austenitic and ferritic stainless steels, with and without Cu addition in 0.05 mol/L NaCl solution

	Austenite		Ferrite	
	With Cu	No Cu	With Cu	No Cu
R_p ($\Omega \text{ cm}^2$)	33028	3974	92145	28358
E_{corr} (mV/SCE)	-222.3	-372.3	-232.5	-236.8
i_{corr} ($\mu\text{A}/\text{cm}^2$)	0.421	3.501	0.150	0.491

Stearn–Geary equation [16], the higher R_p values means the lower values of corrosion current densities.

It is also clear from the polarization curves that the protective effect of Cu on the corrosion of the austenitic stainless steel is predominantly due to inhibition of the anodic reaction (the cathodic currents of both specimens, in a certain potential range, almost coincide). Such anodic inhibiting effect, which is attributed to suppression of the anodic dissolution reaction due to elemental Cu deposition on the steel surface, has been reported by other authors [2–5]. As previously mentioned, the Cu content of each stainless steel specimen has been optimized to give the best antimicrobial activity. The protective ability of the deposited Cu is diminished if it is unstable in a given environment, or if the amount of deposited Cu is not sufficient to protect the steel surface. For the ferritic stainless steel (Fig. 2b), we observe that Cu addition also enhances corrosion resistance, but only in the low anodic potential range. Cu actually degrades the corrosion resistance at higher potentials. It is thus obvious that the stability of the deposited Cu for the ferrite is sensitive to the applied potential, being initially stable at low anodic potentials (<0.2 V vs. SCE) and then unstable when the potential increases beyond this value and the current density exceeds that of the conventional steel. Consequently i_{corr} for both specimens are of the same order of magnitude. Again, Cu addition significantly influences the mechanism of the anodic partial reaction and visibly alters the anodic Tafel slope. Although possible reasons for the harmful effect of Cu include the promotion of the anodic dissolution in the noble potential range where deposited Cu cannot exist as well as the galvanic effect of deposited Cu [2], the actual mechanism is yet to be well understood. Nonetheless, the value of i_{corr} for the Cu-containing specimen is still lower than that of the Cu-free specimen by a factor of 3.

Potential-dependent impedance behavior

The sensitivity of the Cu effect on corrosion performance to applied potential was further investigated by performing variable-potential impedance measurements. The extension of impedance spectroscopy from the potentiostatic to the potential-dependent mode advances the power of interfacial studies by the impedance technique substantially, due to the great amount of information contained in the dependencies of the equivalent electric circuit parameters on potential; the variable of utmost importance in studies of electrode kinetics and reaction mechanisms [17–19]. We have made these measurements in the active anodic region for each specimen. Figure 3 presents the potential dependence of impedance response (in 3D Nyquist and 3D Bode plots) obtained from the austenitic stainless steel specimens

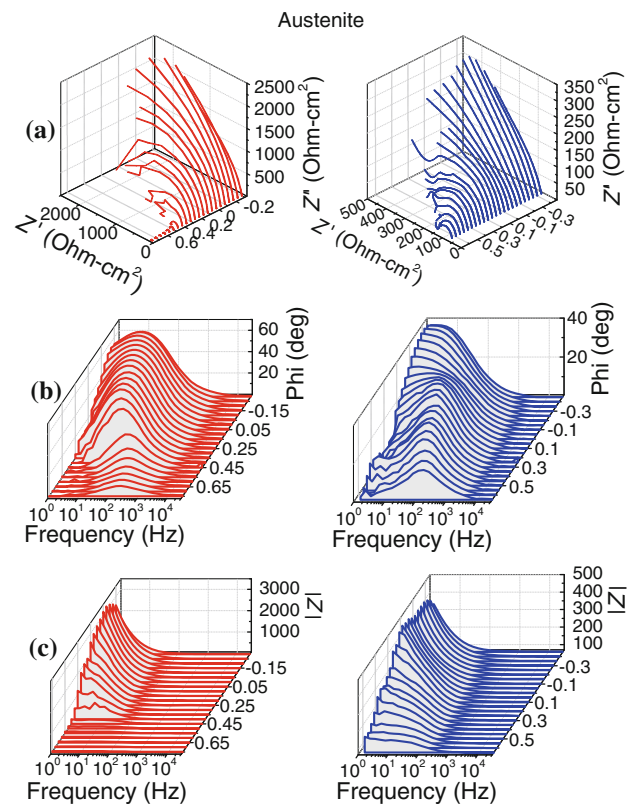


Fig. 3 Impedance spectra of the austenitic stainless steel specimens in 0.05 mol/L NaCl solution (left panels for the Cu-containing specimen, right panels for the Cu-free specimen). Impedance measurements were performed at different potentials

without and with Cu addition in 0.05 mol/L NaCl. Figure 4 gives similar plots for the ferrite specimens. The impedance spectra for the Nyquist plots were adequately analyzed by fitting to the equivalent circuit model $R_s(Q_{dl}R_{ct})$, which comprises a solution resistance R_s , shorted by a constant phase element (CPE) that is placed in parallel to the charge transfer resistance R_{ct} . The value of the charge transfer resistance is indicative of electron transfer across the interface. The use of the CPE, defined by the values Q_{dl} and n , has been extensively described in the literature [20–22] and is employed in the model to compensate for the inhomogeneities in the electrode surface as depicted by the depressed nature of the Nyquist semicircles. The introduction of such a CPE is often used to interpret data for rough solid electrodes. The impedance, Z , of the CPE is [23]

$$Z_{CPE} = Q^{-1}(j\omega)^{-n} \quad (1)$$

where Q and n stand for the CPE constant and exponent, respectively, $j = (-1)^{1/2}$ is an imaginary number, ω is the angular frequency in rad s⁻¹, ($\omega = 2\pi f$) when f is the frequency in Hz. The values of the double layer

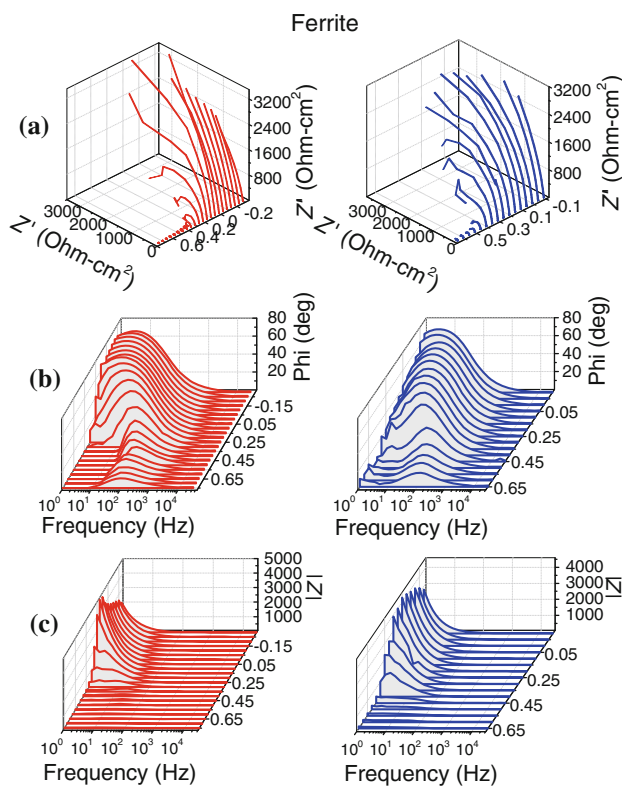


Fig. 4 Impedance spectra of the ferritic stainless steels in 0.05 mol/L NaCl solution (left panels for the Cu-containing specimen, right panels for the Cu-free specimen). Impedance measurements were performed at different potentials

capacitance, C_{dl} , were obtained at the frequency at which the imaginary component of the impedance is a maximum ($-Z''_{max}$) from the equation

$$f(-Z''_{max}) = \frac{1}{2\pi C_{dl} R_t} \quad (2)$$

The values of the electrochemical parameters derived from the Nyquist plots are given in Tables 3 and 4 for the austenite and ferrite, respectively. All of the data confirm a potential dependence of the impedance response for all specimens, which are further illustrated in the resistance-potential plots shown in Fig. 5.

The superior corrosion resistance of the Cu-containing austenitic stainless steel at all potentials is also clearly obvious from Fig. 3, where the impedance parameters are about one order of magnitude higher, with larger capacitive arcs in the Nyquist plots and higher values of the impedance modulus and phase angles from the Bode plots. The effect of Cu on the impedance response of the ferrite is not very pronounced as both specimens (without and with Cu) exhibited remarkably R_{ct} values in the chloride environment, with impedance parameters of similar magnitude. The magnitude of the double layer capacitance (C_{dl}) was always higher for the Cu-containing specimens, suggesting

Table 3 Impedance parameters derived from the Nyquist plots of the austenitic stainless steel specimens in 0.05 mol/L NaCl solution; (a) without Cu (b) with Cu

E (V/SCE)	R_s (Ωcm^2)	C ($\text{F cm}^{-2} \times 10^{-4}$)	n_{sc}	R (Ωcm^2)
a: Without Cu				
-0.30	71.18	4.906	0.6548	1469
-0.25	71.03	5.141	0.6359	1526
-0.20	70.43	5.301	0.6105	1461
-0.15	70.43	5.22	0.6085	1210
-0.10	70.1	4.484	0.611	927.4
-0.05	70.27	3.502	0.6357	769.1
0.00	70.62	2.763	0.662	646.4
0.05	70.91	2.1	0.689	581.2
0.10	70.98	1.718	0.7089	526.8
0.15	71.43	1.361	0.7391	428.4
0.20	71.9	1.067	0.7687	365.2
0.25	71.41	1.104	0.7571	292.1
0.30	71.47	0.9679	0.7734	269.8
0.35	71.63	0.8621	0.787	230.5
0.40	71.84	0.7999	0.7917	224.6
0.45	70.85	0.8627	0.778	197.5
0.50	70.89	0.6928	0.8096	157.8
E (V/SCE)	R_s (Ωcm^2)	C ($\text{F cm}^{-2} \times 10^{-5}$)	n_{sc}	R (Ωcm^2)
b: With Cu				
-0.30	67.95	11.9	0.8	409.7
-0.25	67.98	9.763	0.8	527.5
-0.20	67.91	8.373	0.8	5692
-0.15	67.92	7.40	0.8386	4816
-0.10	68.04	6.508	0.8515	3479
-0.05	68.16	5.618	0.8646	2453
0.00	68.28	4.804	0.8791	1856
0.05	68.43	4.188	0.8909	1538
0.10	68.34	3.831	0.8963	1263
0.15	68.3	3.539	0.8998	1096
0.20	68.12	3.421	0.9001	945.4
0.25	68.18	3.271	0.9023	835.7
0.30	68.2	3.011	0.9116	676.7
0.35	68.37	3.057	0.9089	343.5
0.40	67.55	3.546	0.8894	215.3
0.45	67.32	3.429	0.9051	111.5
0.50	66.6	4.708	0.8722	78.53

that the Cu deposits exert pronounced effects on the stainless steel/solution interface. Since the protectiveness of the Cu does not actually rely on the formation of stable corrosion products, the obtained C_{dl} values can be related to defects in the corrosion product layer. In other words, deposited Cu increased the defect concentration of the layer of corrosion product on the substrate and still

Table 4 Impedance parameters derived from the Nyquist plots of the ferritic stainless steel specimens in 0.05 mol/L NaCl solution; (a) without Cu (b) with Cu

E (V/SCE)	R_s ($\Omega \text{ cm}^2$)	C ($\text{F cm}^{-2} \times 10^{-5}$)	n_{sc}	R ($\Omega \text{ cm}^2$)
a: Without Cu				
-0.10	88.94	6.923	0.8827	13450
-0.05	89.21	5.65	0.895	12320
0.00	89.33	4.237	0.9077	7680
0.05	89.38	3.985	0.9114	7157
0.10	89.37	3.547	0.9133	7590
0.15	89.45	3.141	0.9191	6595
0.20	89.44	2.896	0.9199	5164
0.25	89.08	2.899	0.9114	4587
0.30	89.06	2.652	0.9148	3972
0.35	88.78	2.621	0.9102	2522
0.40	88.26	2.773	0.8989	1477
0.45	87.9	3.171	0.8939	355.9
E (V/SCE)				
R_s ($\Omega \text{ cm}^2$)				
C ($\text{F cm}^{-2} \times 10^{-5}$)				
n_{sc}				
R ($\Omega \text{ cm}^2$)				
b: With Cu				
-0.30	78.1	9.411	0.8587	10520
-0.25	78.07	7.699	0.8681	17860
-0.20	78.11	7.02	0.8733	21840
-0.15	78.13	6.4	0.8782	19940
-0.10	78.05	5.849	0.881	17690
-0.05	78.11	5.163	0.8874	15380
0.00	78.27	4.42	0.8985	13440
0.05	78.34	3.876	0.9036	19650
0.10	78.44	3.417	0.9095	11540
0.15	78.51	3.079	0.915	5347
0.20	78.59	2.788	0.9237	2429
0.25	78	2.928	0.9114	1308
0.30	77.94	2.317	0.9578	443.1
0.35	77.38	1.833	1	192.9

maintained its protective effect. This phenomenon becomes an important consideration in the passive state wherein the oxide layer becomes protective and any increase in defect concentration leads to reduced stability and corrosion resistance as reported in [24].

Certain useful impedance features can be observed as the potential is made more positive: for the austenite we observe that R_{ct} increased initially, albeit slightly, then subsequently decreased steadily with more positive potentials (Fig. 5a). For the Cu-containing specimens, the position of the resistance peaks almost coincide with the free corrosion potentials (E_{corr}) of the specimens, whereas for the Cu-free specimens E_{corr} is more cathodic (~ 0.1 V) than the peak potential. R_{ct} , for the ferrite specimens decreased with increasing potential and this effect for the

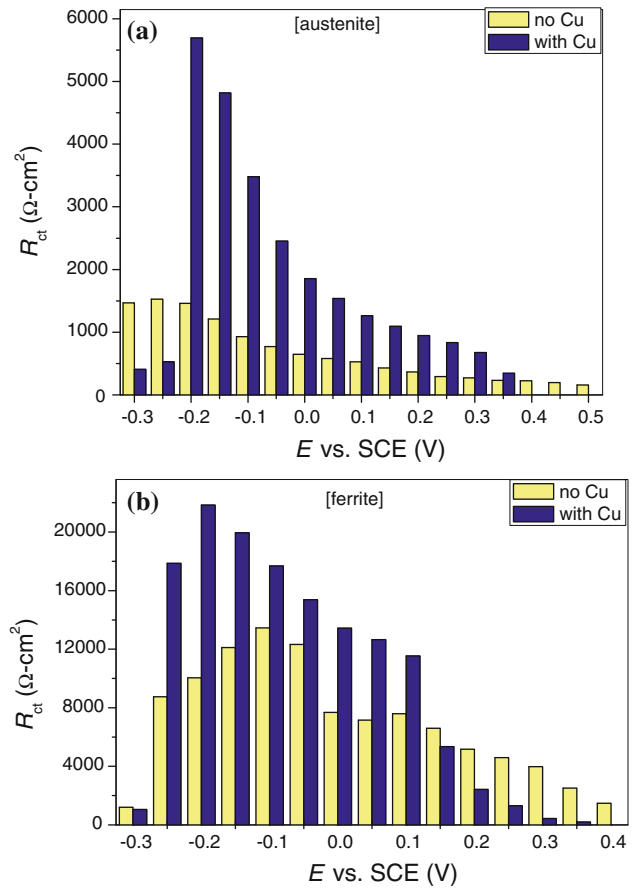


Fig. 5 Potential dependence of charge transfer resistance for **a** austenitic and **b** ferritic stainless steels, with and without Cu addition in 0.05 mol/L NaCl solution

Cu-containing sample becomes especially pronounced beyond 0.1 V, which coincides with the region of sharp increase in corrosion current density as depicted in the polarization curves in Fig. 2, showing consistency of the impedance results with those obtained from potentiodynamic polarization measurements. The existence of resistance peaks can be attributed to electron transfer controlled interfacial reactions where increased propensity for charge transfer at more positive potentials inevitably leads to a decrease in the interfacial resistance. In the case of the Cu-containing specimens, the diminishing protectiveness of deposited Cu as the applied potential becomes more positive can be related to the decreasing stability of the deposited Cu, which gradually undergoes dissolution to Cu^{2+} , possibly yielding CuCl_2^- in the chloride environment [2]:



An interesting finding from Tables 3 and 4 is that the C_{dl} values decreased steadily with increasing potential and display a non-uniform correlation with the charge transfer resistance. On the other hand, the CPE index n increased

steadily with potential (more so for the Cu-containing specimens). This means that variation of potential plays the dominant role in tuning surface charge density, hence the interfacial capacitance. This is understandable, considering that in the absence of concentration polarization as assumed for very dilute solutions, heterogeneous charge transfer is controlled by the change of the reaction rate constant with potential [25]. Another factor to be considered is the complexities involved in the orientation of water molecules near the electrode as the applied potential is varied. The interface interacts more strongly with the oxygen of water when the applied potential is positive thus bringing oxygen nearer to the corroding metal surface. Again, when the applied potential is negative hydrogen is closer to the metal surface and the metal–oxygen distance increases considerably. These effects obviously influence oxidation of the steel substrate and as such control the interfacial properties in a potential dependent manner as observed with the C_{dl} [26].

To further analyze the three-dimensional impedance spectra, we consider the equivalent circuit $R_s(C_{dl}R_{ct})$ which was used to fit the experimental impedance data, as the simplest frame of reference. The impedance (Z) of this circuit is related to the frequency of the signal (f), the charge transfer resistance (R_{ct}), the double layer capacitance of the interface (C), and the resistance of the electrolyte (R_s) by [27]

$$Z = R_s + \frac{R_{ct}}{1 + 2\pi f C R_{ct}} \quad (4)$$

At the high frequency limit the above equation predicts that the impedance of the interface (Z) approaches R_s . This much is obvious from Figs. 3c and 4c, where in the wide frequency range 10^2 – 10^4 Hz, the impedance is reduced to a low and flat plateau, characterizing the solution resistance in the electrochemical response. Again, for any frequency within the low-frequency range (1–10 Hz), the equation predicts that Z approaches the sum of $R_s + R_{ct}$, in which case Z attains values which are orders of magnitude higher than R_s and hence is taken to be virtually equal to R_{ct} . Thus, the modulus–potential relationship exhibits parabolic character with an impedance summit and the impedance modulus response is restricted to low frequencies and disappears completely for the Cu-bearing specimens at high potentials.

The phase angle peaks shift from low to medium frequencies with corresponding diminution of the peak heights. Also, there is no response at high frequencies for all specimens, while the low-frequency peaks disappear at high potentials for the Cu-containing specimens. Thus, besides the obvious improvement in corrosion resistance resulting from Cu addition, the observed absence of any impedance response at high potentials represents another important

effect of Cu on the corrosion behavior of both austenitic and ferritic stainless steels in 0.05 mol/L NaCl solution.

Conclusions

We investigated the influence of Cu addition on the electrochemical corrosion behavior of stainless steels in 0.05 mol/L NaCl by means of potentiodynamic polarization and variable-potential impedance measurements. Cu addition significantly improved the corrosion resistance of the austenite in the studied potential range, whereas the protective effect is restricted to low anodic potentials for the ferrite. Consistent with the polarization experiments, impedance parameters also varied with applied potential, showing characteristic peak potentials for the resistance and impedance modulus, while the double layer capacitance decreased steadily with potential. Our findings support the view that three-dimensional presentation of potential-dependent impedance data affords a fuller description of the complex interfacial processes involved in the electrochemical corrosion phenomenon.

Acknowledgements E.E. Oguzie is a TWAS-UNESCO associate.

References

1. Zhang Z, Liu G, Jiang LZ (2008) Mater Chem Phys 111:238
2. Ujiro T, Satoh S, Staehle RW, Smyrl WH (2001) Corros Sci 43:2185
3. Pardo A, Merino MC, Coy AE, Arrabal R, Viejo F, M'hich A (2007) Appl Surf Sci 253:9164
4. Lin HT, Tsai WT, Lees JT, Huang CS (1992) Corros Sci 33:691
5. Dan ZG, Ni HW, Xu BF, Xiong J, Xiong PY (2005) Thin Solid Films 492:93
6. Zhang ZX, Lin G, Xu Z (2008) J Mater Proc Technol 205:419
7. Amin MA, Abd El Rehim SS, El-Naggar MM (2009) J Mater Sci 44:6258. doi:[10.1007/s10853-009-3856-2](https://doi.org/10.1007/s10853-009-3856-2)
8. Niu L, Yin YH, Guo WK, Lu M, Qin R, Chen S (2009) J Mater Sci 44:4511. doi:[10.1007/s10853-009-3654-x](https://doi.org/10.1007/s10853-009-3654-x)
9. Rao VS, Singhal LK (2009) J Mater Sci 44:2327. doi:[10.1007/s10853-008-2976-4](https://doi.org/10.1007/s10853-008-2976-4)
10. Wen DC (2009) J Mater Sci 44:6363. doi:[10.1007/s10853-009-3877-x](https://doi.org/10.1007/s10853-009-3877-x)
11. Yang K, Lu M (2007) J Mater Sci Technol 23:333
12. Lu M, Chen S, Dong J, Yang K (2005) Chin J Mater Res 19:581
13. Yang K, Chen S, Dong J, Lu M (2005) Metall Funct Mater 12:6
14. Banas J, Mazurkiewicz A (2000) Mater Sci Eng A277:183
15. Mansfeld F (2009) J Solid State Electrochem 13:515
16. Stearn M, Geary AL (1957) J Electrochem Soc 104:56
17. Ragoisha GA, Bondarenko AS (2005) Electrochim Acta 50:1553
18. Darowicki K, Orlikowski J, Aratunow A (2004) J Solid State Electrochem 8:352
19. Darowicki K, Kawula J (2007) J Solid State Electrochem 43:1055
20. Lopez DA, Simison SN, de Sanchez SR (2003) Electrochim Acta 48:845

21. William Grips VK, Selvi VE, Barshilia HC, Rajam KS (2006) *Electrochim Acta* 51:3461
22. Behpour M, Ghoreishi SM, Gandomi-Naisar A, Soltani N, Salavati-Niasari M (2009) *J Mater Sci* 44:2444. doi:[10.1007/s10853-009-3309-y](https://doi.org/10.1007/s10853-009-3309-y)
23. Harek Y, Larabi L (2004) *Kem Ind* 53:55
24. Postrach B, Garz I, Strehblow HH (1994) *Mater Corros* 45:508
25. Bisquert J, Randriamahazaka H, Garcia-Belmonte G (2005) *Electrochim Acta* 51:627
26. Krishnan CV, Garnett M (2006) *Electrochim Acta* 51:1541
27. Sayed SY, El-Deab MS, El-Anadouli BE, Ateya BG (2003) *J Phys Chem B* 107:5575